Wafer Level Vacuum Packaged Out-of-Plane and In-Plane Differential Resonant Silicon Accelerometers for Navigational Applications

Illhwan Kim, Seonho Seok, Hyeon Cheol Kim, Moon Koo Kang, and Kukjin Chun

Abstract—**Inertial-grade vertical-type and lateral-type differential resonant accelerometers (DRXLs) are designed, fabricated using one process and tested for navigational applications. The accelerometers consist of an out-of-plane (for z-axis) accelerometer and in-plane (for x, y-axes) accelerometers. The sensing principle of the accelerometer is based on gap-sensitive electrostatic stiffness changing effect. It says that the natural frequency of the accelerometer can be changed according to an electrostatic force on the proof mass of the accelerometer.**

The out-of-plane resonant accelerometer shows bias stability of 2.5 μg, sensitivity of 70 Hz/g and bandwidth of 100 Hz at resonant frequency of 12 kHz. The in-plane resonant accelerometer shows bias stability of 5.2 μg, sensitivity of 128 Hz/g and bandwidth of 110 Hz at resonant frequency of 23.4 kHz. The measured performances of two accelerometers are suitable for an application of inertial navigation.

Index Terms—**MEMS, accelerometer, resonant, inertial-grade, differential, out-of-plane, in-plane, vacuum packaging, wafer-level**

I. INTRODUCTION

MEMS accelerometers are categorized into piezoresistive-type accelerometers, capacitive-accelerometers, and resonant-type accelerometers based on sensing principle. Piezoresistive-type accelerometers have advantages of simple process and low cost but have poor resolution, accuracy and sensitivity to temperature variations. Capacitive-type accelerometers are insensitive to temperature variations, easy for interfacing with circuit and has better resolution and accuracy than piezoresistive-type. Both have output form of voltage, but resonant-type has output form of frequency. It also has the highest resolution and accuracy among them, but the system is the most complex among them. Some of them are reported to have good performances comparable to those of the conventional mechanical systems. The developed MEMS accelerometer is generally fabricated by capacitive type [1-7]. Recently, resonant-type accelerometers have been reported [8-10]. Resonant sensors have many advantages over the conventional capacitive type: wide dynamic range, quasi-digital nature of the output signal, and the inherent continuous self-test capability. Time is by far the best measurand. Furthermore, the upper bound of the dynamic range is limited by the measurement time: increasing the measurement time automatically results in a larger dynamic range. The digital output signal can be directly connected to digital signal processing electronics. Analog to digital conversion is not necessary. Furthermore, a frequency signal can be transported over long distances with no loss of accuracy.

Quartz-based resonant accelerometers also known as vibrating beam accelerometers (VBA) have been fabricated to implement the resonant accelerometers because of the stable properties of quartz. It senses acceleration by measuring the change in the resonant frequency of beam oscillations under the inertial loading of a proof mass. Its piezoelectric characteristic makes driving and signal sensing easier. Silicon MEMS resonant accelerometer follows the VBA. The silicon MEMS process offers several advantages over quartz that enables superior accelerometer design features [11]:

(1) Semiconductor-grade, single-crystal silicon is a

Manuscript received January 5, 2005; revised March 10, 2005

School of Electrical Engineering and Computer Sciences Seoul National University
E-mail: cliffman@mintlab.snu.ac.kr

perfectly elastic structural material that can be produced with extremely low levels of impurities.

(2) The MEMS process enables fabrication of very small (millimeter scale in the case of the conventional MEMS silicon accelerometer) resonator elements that are well isolated from the influence of parasitic instrument package stress.

(3) Capacitively based, electrostatic resonator actuation and sensing that offers greater design flexibility than the piezoelectric quartz technology.

MEMS silicon resonant accelerometer needs the vacuum environment for a linear, stable oscillation compared to quartz-based resonant accelerometer because of degrading of the quality factor of the mechanical resonator by the dampness of air. Hence, the wafer level vacuum packaging technique is one of the important technologies for commercialization of inertial sensors.

To develop inertial-grade MEMS silicon accelerometer, the novel differential resonant accelerometer (DRXL) is designed, fabricated and tested. The two different DRXLs are fabricated using same process with single crystal silicon. One of them can detect the vertical acceleration and the other can detect the lateral acceleration. Therefore, 3-DOF (Degree Of Freedom) can be detected with these accelerometers. To fabricate the accelerometer using single crystal silicon, a novel fabrication process is developed. The fabricated accelerometers are measured to evaluate the performance. The measured results show the performance suitable to inertial-grade.

II. Design

1. Out-of-Plane DRXL

The out-of-plane DRXL consists of one proof mass with torsional spring and two torsional resonators. The torsional resonators are adopted to use differential driving scheme that makes the displacement of resonator depend on the driving voltage linearly. The proof mass of the DRXL is also implemented in a torsional type because the acceleration is to be detected differentially using two separate resonators. The mathematical modeling of the accelerometer introduced in this section. The schematic diagram with design parameters is illustrated in Fig. 1.

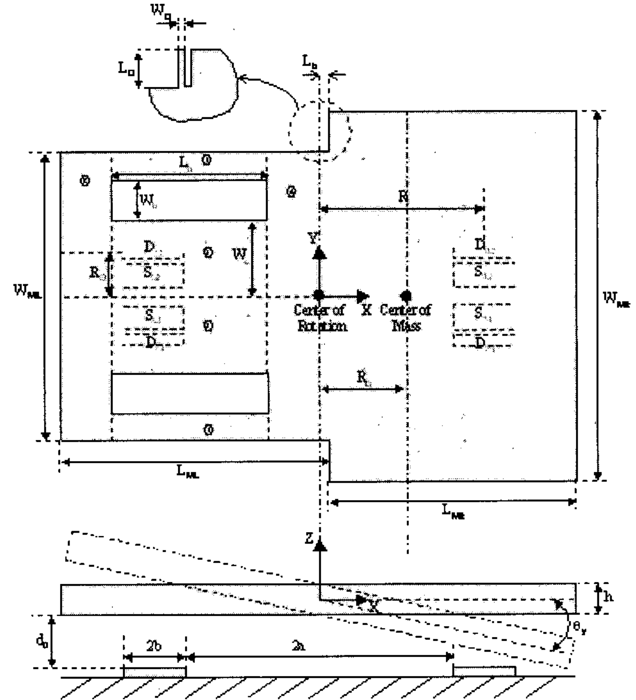

Fig. 1. Schematic diagram of out-of-plane DRXL

A dimension of DRXL is expanded to 2500 μm by 1900 μm. The location of resonator on proof mass is crucial for high sensitive accelerometer. Considering the reliability of mechanical structure, the resonator is placed to 800 μm away from center of rotation.

With the modified structure, the mathematical modeling is described below. The displacement angle of outer proof mass is given by equation (1).

$$\theta_y = \frac{\tau(g)}{k_{y_eff}} = \frac{(M_R + M_L) g R_G}{k_y - \frac{2}{3}\frac{\varepsilon_0 A_T V_T^2 (3a^2 + 6ab + 4b^2)}{d_0^3}} \tag{1}$$

From equation (1), the angle is proportional to mass of proof mass and the distance between center of mass and center of rotation. It also depends on the location of resonator in proof mass.

For mechanical resonator, the electrostatic stiffness is given by equation (2).

$$\begin{aligned} k_{x_eL} &\cong -\frac{1}{3}\cdot\frac{\varepsilon_0 A_T V_T^2 R_D^2}{[d_0 + (a+b)\theta_y]^3}\cdot\left\{1 + 2\left(\frac{b\theta_y}{d_0 + (a+b)\theta_y}\right)^2\right\} \\ k_{x_eR} &\cong -\frac{1}{3}\cdot\frac{\varepsilon_0 A_T V_T^2 R_D^2}{[d_0 - (a+b)\theta_y]^3}\cdot\left\{1 + 2\left(\frac{b\theta_y}{d_0 - (a+b)\theta_y}\right)^2\right\} \end{aligned} \tag{2}$$

Using equation (2), output frequency is given by equation (3).

$$f_{xL}-f_{xR}=\frac{1}{2\pi}\sqrt{\frac{k_x+k_{x_eL}}{I_x}}-\frac{1}{2\pi}\sqrt{\frac{k_x+k_{x_eR}}{I_x}}$$

$$=\frac{1}{2\pi}\sqrt{\frac{k_x}{I_x}}\left(\sqrt{1+\frac{k_{x_eL}}{k_x}}-\sqrt{1+\frac{k_{x_eR}}{k_x}}\right)=\frac{1}{2\pi}\sqrt{\frac{k_x}{I_x}}\left(K_1\theta_y+K_3\theta_y^3+\dots\right)$$

$$K_1=\frac{\varepsilon_0 A_T V_T^2 R_T^2(a+b)}{d_0^4 k_x\sqrt{1-\frac{\varepsilon_0 A_T V_T^2 R_T^2}{3d_0^3 k_x}}} \tag{3}$$

where $K_3=\frac{\varepsilon_0 A_T V_T^2 R_T^2(a+b)}{8\left(3d_0^4 k_x-\varepsilon_0 d_0 A_T V_T^2 R_T^2\right)^3}$

$$\times\begin{Bmatrix}720\left(a^2+2ab+2b^2\right)d_0^6 k_x^2\\ -24\left(11a^2+22ab+28b^2\right)\varepsilon_0 d_0^3 k_x A_T V_T^2 R_T^2\\ +7\left(5a^2+10ab+13b^2\right)\varepsilon_0 A_T^2 V_T^4 R_T^4\end{Bmatrix}$$

In equation (3), coefficient K_1 is related with the sensitivity of out-of-plane accelerometer and coefficient K_3 is associated with the non-linearity of the accelerometer.

The modal analysis of designed DRXL was performed by using ANSYS simulation. It is known that the proof mass has lower frequency to be sensitized the external acceleration and the resonators have higher frequency to be decoupled with the proof mass from the modal analysis. The resonant frequencies of resonator and proof mass are 15.916 kHz and 1.068 kHz respectively.

The output characteristics simulated by using Matlab are shown in Fig. 2 for each resonator and differential mode. For each condition, the amplitude of ac signal is assumed to 100 mV.

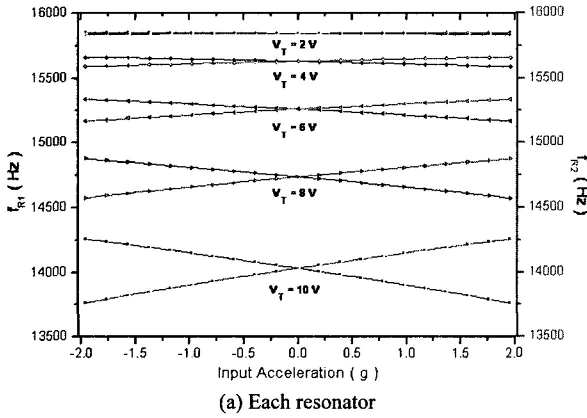

(a) Each resonator

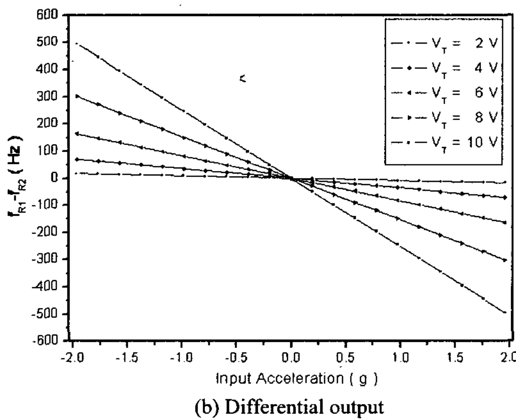

(b) Differential output

Fig. 2. Resonant frequency change of resonators for out-of-plane DRXL

2. In-Plane DRXL

The in-plane DRXL is composed of a resonator and two proof masses to implement differential scheme. The resonator is double-ended tuning fork (DETF) type that has a proof mass for each beam of DETF. The sensing electrodes with the type of parallel plate are inserted between proof mass and resonator to cause a gap sensitive electrostatic stiffness changing effect. The proposed structure consists of two independent mechanical systems; mechanical coupling between two systems does not exist, but electrical coupling may exist in this system. The schematic diagram with design parameters is illustrated in Fig. 3.

Simplified model is used to derive the equation of motion for in-plane DRXL. It is composed of one proof mass and one resonator for convenience and bias voltages for each electrode are illustrated as shown Fig. 4. The sensing dc voltage is applied to proof mass and the dc voltage and complementary ac voltage are used to vibrating the resonator in its natural frequency. The resonator is biased to ground.

The governing equation of in-plane DRXL is given by

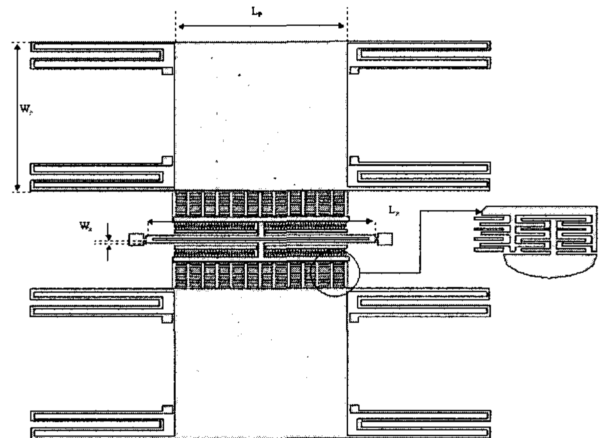

Fig. 3. Schematic diagram of in-plane DRXL

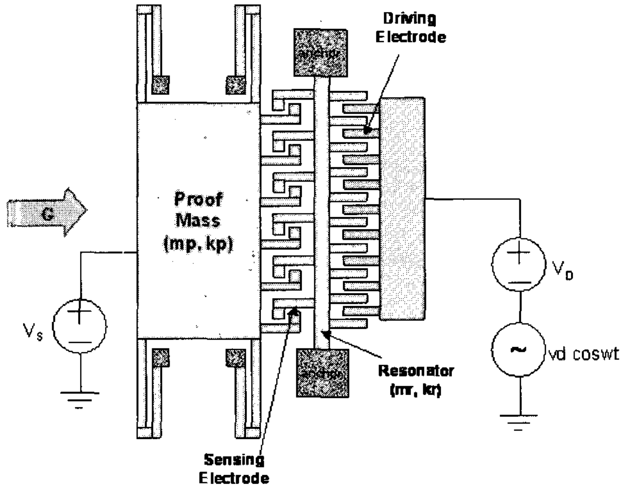

Fig. 4. Simplified model for in-plane DRXL

$$M_r\ddot{x}+c\dot{x}+k_{mr}x=F_e+F_a \tag{4}$$

M_r: mass of resonator, c: damping coefficient, k_{mr}: mechanical spring constant of resonator, F_a: acceleration force (= $m_r a$), F_e: electrostatic force by sensing and driving electrodes

The total electrostatic force generated from sensing and driving electrodes in the lateral resonator is given by

$$\begin{aligned}F_e &= F_s+F_d\\ &=\frac{1}{2}\frac{\varepsilon_0 A_s V_s^2}{(d_{0p}-x_g)^2}+\frac{1}{2}\frac{\varepsilon_0 h V_d^2}{d_{0c}}\\ &=\frac{1}{2}\frac{\varepsilon_0 A_s V_s^2}{(d_{0p}-x_g)^2}+\frac{1}{2}\frac{\varepsilon_0 h}{d_{0c}}(V_D+v_d\cos\omega_r t)^2\\ &=\frac{1}{2}\frac{\varepsilon_0 A_s V_s^2}{(d_{0p}-x_g)^2}+\frac{1}{2}\frac{\varepsilon_0 h}{d_{0c}}(V_D^2+2V_D v_d\cos\omega_r t+v_d^2\cos^2\omega_r t)\\ &=\frac{1}{2}\frac{\varepsilon_0 A_s V_s^2}{(d_{0p}-x_g)^2}+\frac{\varepsilon_0 h V_D^2}{2d_{0c}}+\frac{\varepsilon_0 h v_d^2}{4d_{0c}}+\frac{\varepsilon_0 h V_D v_d}{d_{0c}}\cos\omega_r t+\frac{\varepsilon_0 h v_d^2}{4d_{0c}}\cos 2\omega_r t\end{aligned} \tag{5}$$

where x_g is total displacement of sensing gap

The electrostatic force applied to this accelerometer is composed of gap sensitive force, voltage dependent force, and sinusoidal force to vibrating the resonator. Among these forces, the gap sensitive force is used to sense the acceleration because the force cause an electrostatic stiffness change according to external acceleration as mentioned before. Therefore, the electrostatic stiffness of this accelerometer is dependent on the displacement of proof mass and resonator and given by

$$k_e=-\frac{\varepsilon_0 A_s V_s^2}{(d_0-x_g)^3} \tag{6}$$

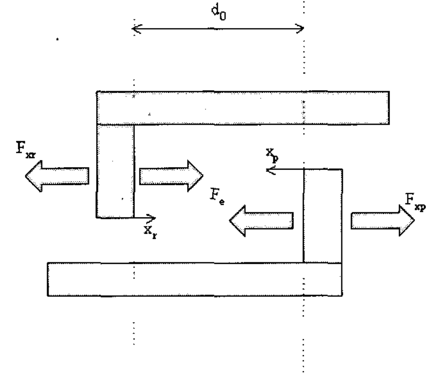

Fig. 5. Exploded view of one of sensing electrodes

The displacement of sensing gap d_0 is critical to the accelerometer performance such as sensitivity and linearity. The one of sense electrodes is illustrated in Fig. 5.

The equations among forces exerted on sense electrodes are known from this figure.

$$\begin{aligned}x_g &= x_r+x_p\\ k_{er}x_r &= k_{ep}x_p\end{aligned} \tag{7}$$

where x_r is displacement of resonator, x_p is displacement of proof mass, and k_{er} and k_{ep} are electrostatic stiffness by dc voltage on sense and drive electrodes

The displacement of sensing gap x_g is calculated from two equations.

$$x_g=\left(\frac{k_{er}}{k_{ep}}+1\right)\frac{g}{\omega_{er}^2} \tag{8}$$

Therefore, the effective resonant frequency of single resonator is given by

$$\begin{aligned}f_{effr} &= \frac{1}{2\pi}\sqrt{\frac{k_{mr}+k_e}{M_r}}=f_0\sqrt{1+\frac{k_e}{k_{mr}}}\\ &\approx f_0\left(1+\frac{k_e}{2k_{mr}}\right)=f_0+\frac{\varepsilon_0 A_s V_s^2 f_0}{2k_{mr}}\frac{1}{(d_0-x_g)^3}\end{aligned} \tag{9}$$

The resonant frequency of resonator is proportional to 1/g3. The nonlinear frequency output of each resonator can be linear with input acceleration as follows.

$$\begin{aligned}f_{out} &= f_{effR}-f_{effL}\\ &=\frac{\varepsilon_0 A_S V_S^2 f_0}{2k_{mr}}\left[\frac{1}{(d_0-x_g)^3}-\frac{1}{(d_0+x_g)^3}\right]\\ &=\frac{3\varepsilon_0 A_S V_S^2 f_0}{k_{mr}d_0^4}x_g+\frac{\varepsilon_0 A_S V_S^2 f_0}{k_{mr}d_0^6}x_g^3\end{aligned} \tag{10}$$

$$= \frac{3\varepsilon_0 A_S V_S^2 f_0}{k_{mr} d_0^4}\left(\frac{k_{er}}{k_{ep}}+1\right)\frac{1}{\omega_{er}^2} g + \frac{\varepsilon_0 A_S V_S^2 f_0}{k_{mr} d_0^6}\left(\frac{k_{er}}{k_{ep}}+1\right)^3 \frac{1}{\omega_{er}^6} g^3$$
$$= K_{x1} g + K_{x3} g^3$$

As is out-of-plane DRXL, the coefficient K_{x1} related to input acceleration g is called as sensitivity of the in-plane DRXL and the coefficient K_{x3} related to g^3 makes an effect to the linearity of the in-plane DRXL. These two parameters should be adjusted well to design high performance accelerometer system.

The modal analysis for proof mass and resonator is performed using ANSYS. The mechanical resonant frequencies for a proof mass and resonator are 3.926 kHz and 28.204 kHz respectively.

The frequency output characteristics for each resonator and differential mode are presented in Fig. 6. For each condition, the amplitude of ac signal is assumed to 100 mV.

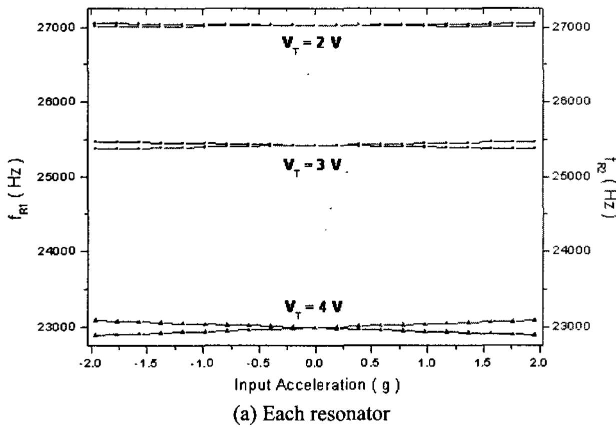

(a) Each resonator

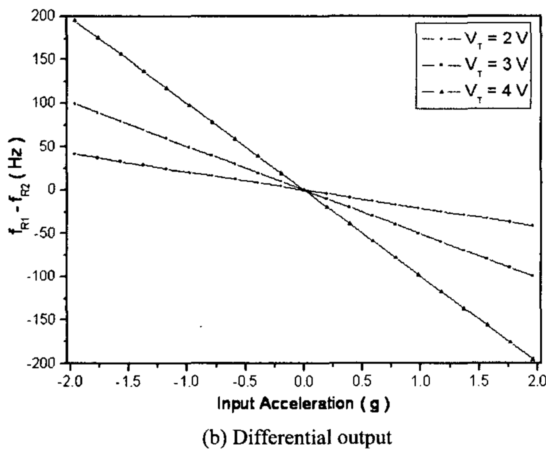

(b) Differential output

Fig. 6. Resonant frequency change of in-plane DRXL

III. FABRICATION

A novel micromachining process is developed to use single crystalline silicon as structure layer due to its better mechanical properties than of polysilicon. The process is called mixed micromachining process because it uses surface micromachining process as well as bulk micromachining process. The mixed micromachining process is shown in Fig. 7. And the SEM pictures of out-

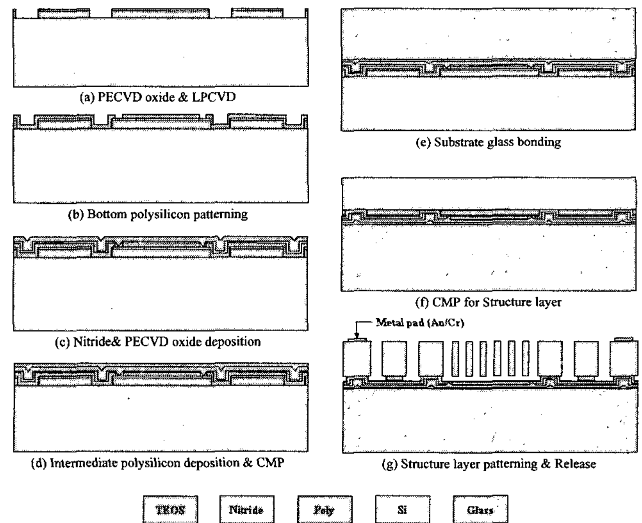

Fig. 7. Process sequences for the fabrication of DRXLs. (a) 2 um-thick PECVD oxide & 0.2 um-thick LPCVD nitride patterning, (b) 0.5 um-thick bottom polysilicon patterning, (c) Nitride (0.2um) & PECVD oxide (1 um) deposition, (d) Intermediate polysilicon deposition & CMP, (e) Substrate glass bonding, (f) CMP for structure layer (40 um), and (g) Structure layer patterning & Release

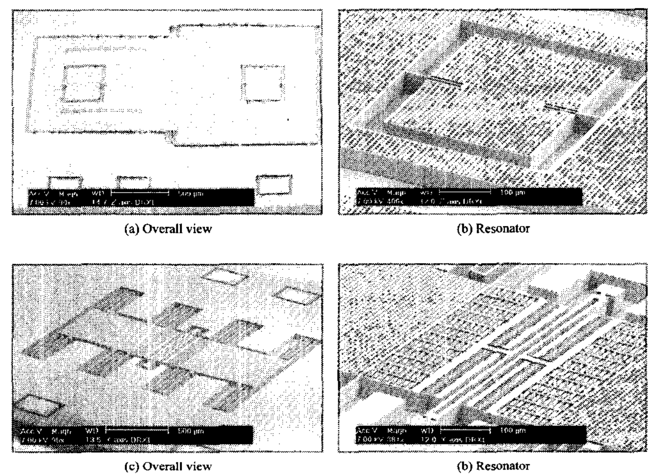

Fig. 8. SEM pictures of the fabricated DRXLs. (a) Overall view of out-of-plane DRXL, (b) Resonator of out-of-plane DRXL, (c) Overall view of in-plane DRXL, (d) Resonator of in-plane DRXL

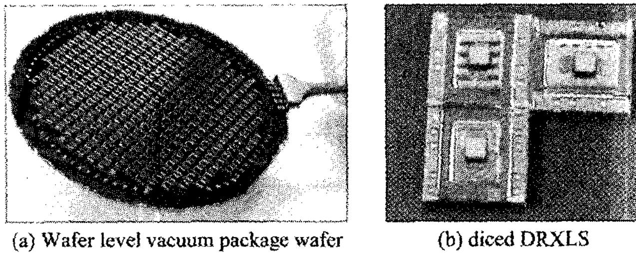

(a) Wafer level vacuum package wafer (b) diced DRXLS

Fig. 9. Vacuum packaged DRXLs

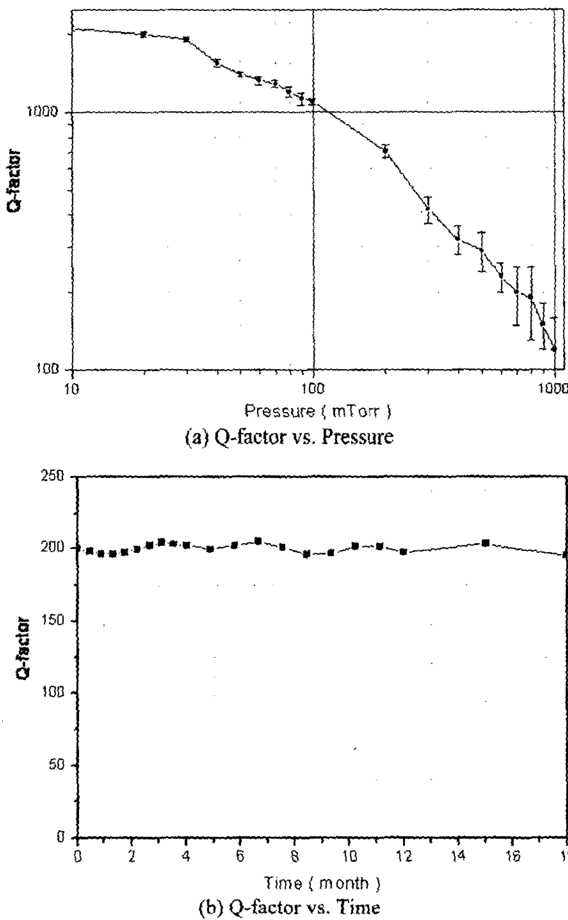

(a) Q-factor vs. Pressure

(b) Q-factor vs. Time

Fig. 10. Measurement results of vacuum packaging

of-plane DRXL and in-plane DRXL are shown in Fig. 8.

After releasing the structure, the silicon wafer is anodically bonded with a glass cap wafer for wafer level vacuum packaging. The glass sealing-cap is fabricated using HF wet etching. The wafer level vacuum packaged devices and diced out-of-plane and in-plane accelerometers are shown in Fig. 9.

The DRXL with signal processing circuit is placed in the vacuum chamber and the pressure in the chamber is changed using pump. The resonator is driven by using DC voltage and ac small signal. And then, the output signal of DRXL is monitored by dynamic signal analyzer. The relationship between Q-factor and pressure level is extracted from the measured output signal. The resultant graph is also presented in Fig. 10 (a) for in-plane accelerometer. The quality factor is monitored to estimate the stability of the vacuum level using measurement setup as above shown. The measurement has been performed for one and a half years. The measured result is shown in Fig. 10 (b).

IV. MEASUREMENT

Signal processing unit for DRXLs consists of sensing parts (charge amplifier, high pass filter, amplifier) and driving parts (phase shifter, rectifier, comparator, amplifier) as shown in Fig. 11.

The fabricated DRXLs are tested by applying the gravitational force of -1 g, 0 g, 1 g. For out-of-plane DRXL, the resonator in heavier side of proof mass shows sensitivity of 45 Hz/g at nominal frequency of 12 kHz. And the resonator in lighter side of proof mass shows sensitivity of 25 Hz/g at nominal frequency of 12.5 kHz as shown in Fig. 12. Therefore, the differential output between two resonators shows 70 Hz/g. The mechanical quality factor of this device is about 200.

For in-plane DRXL, one resonator shows sensitivity of 64 Hz/g at nominal frequency of 23.4 kHz and the other resonator shows sensitivity of 64 Hz/g at nominal frequency of 33.4 kHz as shown in Fig. 13. Therefore, the differential output between two resonators shows 128 Hz/g. The mechanical quality factor is about 200.

The output frequency fluctuation is important factor to

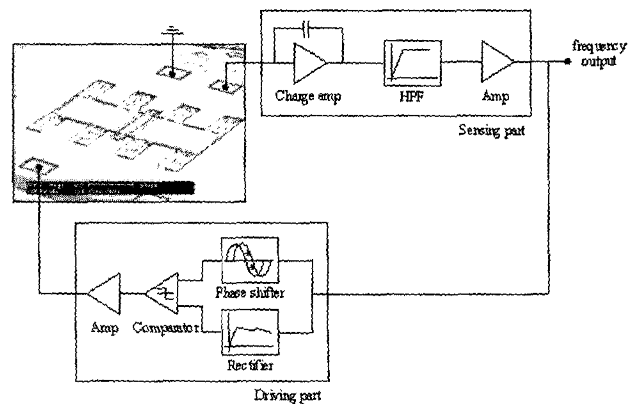

Fig. 11. Signal-processing unit for DRXLs

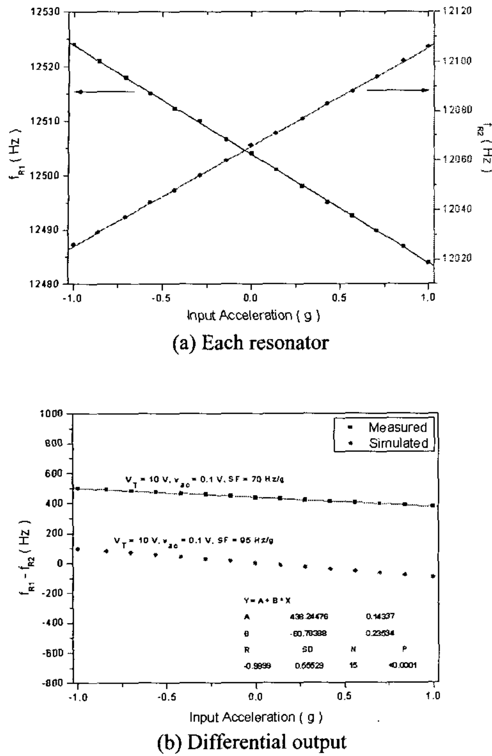

(a) Each resonator

(b) Differential output

Fig. 12. Measured output of out-of-plane DRXL

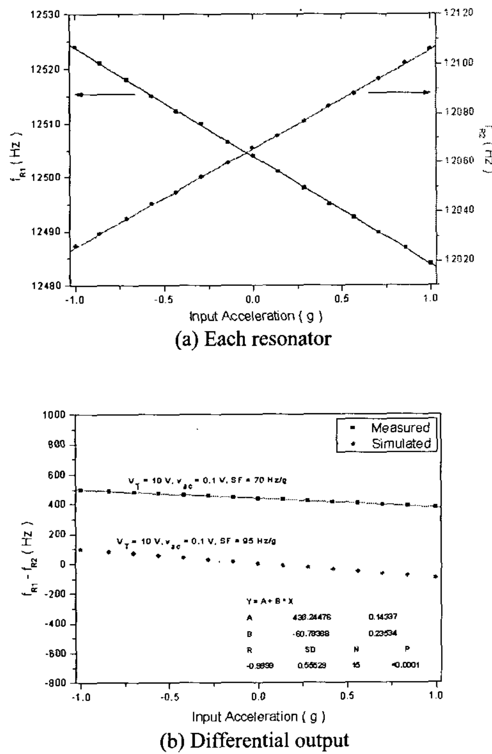

(a) Each resonator

(b) Differential output

Fig. 13. Measured output of in-plane DRXL

determine the resolution of DRXL, so the Allan variance is measured using SR(Stanford Research)620 frequency counter. The measured result is shown in Fig. 14. The

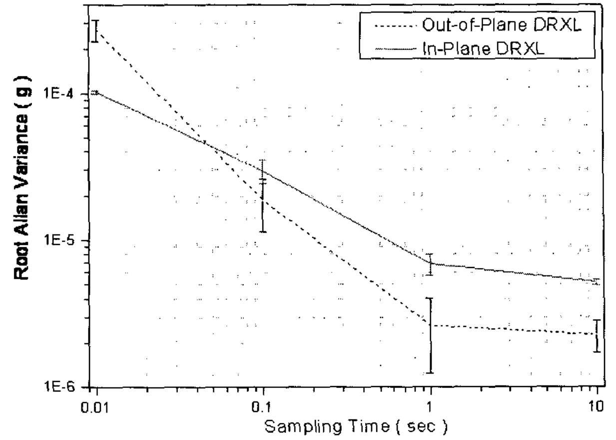

Fig. 14. Measured Allan Variance

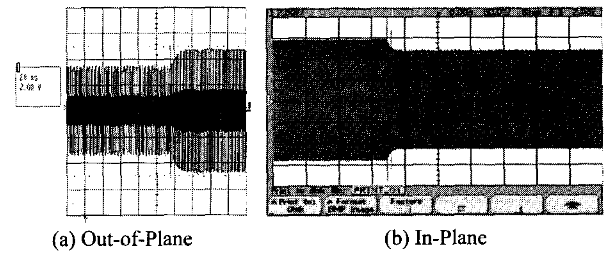

(a) Out-of-Plane (b) In-Plane

Fig. 15. Measured bandwidth of DRXLs

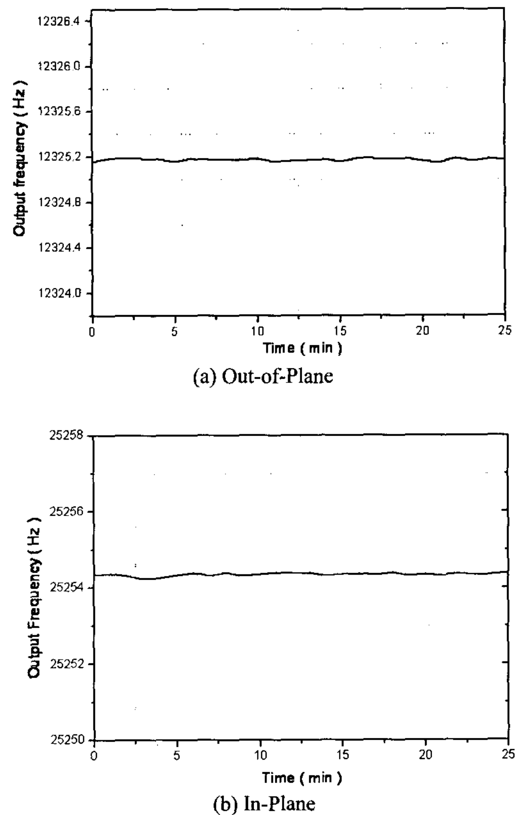

(a) Out-of-Plane

(b) In-Plane

Fig. 16. Measured bias stability of DRXLs

Table. 1. Measured performance of DRXLS

Performance Parameter	Out-Of-Plane DRXL	In-Plane DRXL
Resonant Frequency (kHz)	12/12.5	23.4/33.4
Sensitivity (Hz/g)	70	128
Bias Stability (μg)	2.5	5.2
Bandwidth (Hz)	100	110
Frequency Stability (ppb)	50	290

resonant frequency is measured at a different sampling time; 0.01 sec, 0.1 sec, 1 sec, 10 sec. At each sampling time, the frequency is measured 5 times repetitively and averaged. As the sampling time larger, the Allan variance converges a certain value as shown in Fig. 14.

The bandwidths of DRXLs are also important parameter, so it is measured by applying a step function electrically to proof mass of the accelerometer. The measured output signals for DRXLs are shown in Fig. 15. The estimated bandwidths are about 100 Hz for both DRXLs.

The output frequency of the out-of-plane DRXL and the in-plane DRXL is gathered using HP 53132A frequency counter for 25 minutes at the condition of 0.01 sec gate time. The measured results are shown in Fig. 16. In the out-of-plane DRXL, it has an average of 12325.17 Hz and a standard deviation of 11.9 mHz and the bias stability is 155 μg which is given by dividing the standard deviation by scale factor. And the in-plane DRXL has an average of 25254.35 Hz and a standard deviation of 42.4 mHz and the bias stability is 330 μg. The measured performance parameters are summarized in Table 1.

V. CONCLUSIONS

To achieve micro-g resolution, resonant sensing principle using gap-sensitive electrostatic stiffness changing effect is adopted. Out-of-plane accelerometer and in-plane accelerometer are implemented in differential type that cancels the common noise components on each resonator, which improves noise performances of accelerometers. Each component of out-of-plane accelerometer is implemented with torsional moving structures to use the advantages of differential scheme. In-plane accelerometer consists of a pair of resonator-proof mass. Therefore, each pair senses an external acceleration independently.

A novel fabrication process using (111) single crystalline silicon and glass substrate is developed to fabricate the designed accelerometers. In-plane and out-of-plane accelerometers are simultaneously fabricated using the same fabrication process.

To estimate the performance of DRXLs, signal-processing board is made using charge amplifier. The Allan variances are measured to evaluate the resolution of two fabricated DRXLs. The measurement results show a bias stability of 2.5 μg for out-of-plane accelerometer and a bias stability of 5.2 μg for in-plane accelerometer, which shows the developed two DRXLs are applicable to inertial navigation/guidance area. MEMS accelerometers using capacitive and resonant sensing mechanism were reported that they had a resolution of a few micro-g. And they were fabricated by using complex process to implement micro-g noise level. However, the fabricated DRXLs have a bias stability of a few micro-g. It means that the performance of the developed DRXLs is much higher than the previously reported accelerometers. And the fabrication process is suitable for batch fabrication because the process is performed in wafer level with wafer level release, wafer level vacuum packaging.

REFERENCES

[1] H. Luo, G. Zhang, L. Richard and G. K. Fedder, "A Post-CMOS Micromachined Lateral Accelerometer," *Journal of Microelectromechanical systems*, Vol. 11, No. 3, pp.188-195, June 2002.

[2] J. Chae, H. Kulah and K. Najafi, "A Monolithic Three-axis Silicon Capacitive Accelerometer with Micro-G Resolution," *The 12th International Conference on Solid State Sensors, Actuators and Microsystems (Transducers '03)*, Boston, pp.81-84, June 8-12, 2003.

[3] H. Kulah, J. Chae and K. Najafi, "Noise Analysis and Characterization of a Sigma-Delta Capacitive Silicon Accelerometer," *The 12th International Conference on Solid State Sensors, Actuators and Microsystems (Transducers '03)*, Boston, USA, pp.95-98, June 8-12, 2003.

[4] N. Yazdi and K. Najafi, "An All-Silicon Single-Wafer Micro-g Accelerometer with a Combined Surface and Bulk Micromachining Process," *Journal of Microelectromechanical systems*, Vol. 9, No. 4, pp. 544-550, Dec. 2000.

[5] J. Chae, H. Kulah and K. Najafi, "An In-plane High-Sensitivity, Low-noise Micro-G Silicon Accelerometer," *IEEE the 6th Annual International Conference on Micro Electro Mechanical System (MEMS'03)*, Kyoto, Japan,

pp.466-469, Jan. 19-23, 2003.

[6] H. Takao, H. Fukumoto and M. Ishida, "A CMOS Integrated Three-Axis Accelerometer Fabricated with Commercial Submicrometer CMOS Technology and Bulk-Micromachining," *IEEE Transaction on Electron Devices*, Vol. 48, No. 9, pp.1961-1968, Sep. 2001.

[7] H. Takao, Y. Matsumoto and M. Ishida, "A Monolithically Integrated Three Axial Accelerometer Using Stress Sensitive CMOS Differential Amplifiers," *The 9th International Conference on Solid State Sensors, Actuators and Microsystems (Transducers'97)*, Chicago, USA, 1997, pp.1173-1176, June 16-19.

[8] D. W. Burns, R. D. Horning, W. R. Herb, J. D. Zook, and H. Guckel, "Resonant microbeam accelerometer," *The 8th International Conference on Solid-State Sensors and Actuators, and Eurosensors IX (Transducers'95)*, Stockholm, Sweden, 1995, pp.659-662, June 25-29.

[9] T. V. Rozhart, H. Jerman, J. Drake, and C. de Cotiis,"An inertial-grade, micromachined vibrating beam accelerometer," *The 8th International Conference on Solid-State Transducers and Actuators, and Eurosensors IX (Transducers'95)*, Stockholm, Sweden, 1995, pp.656-658, June 25-29.

[10] M. Helsel, G. Gassner, M. Robinson and J. Woodruff, "A Navigation Grade Micro-Machined Silicon Accelerometer," *IEEE Position Location and Navigation Symposium*, pp.51-58, April 11-15, 1994.

[11] R. E. Hopkins, J. T. Borenstein, B. M. Antkowiak, P. A. Ward, R. D. Elliot, M. S. Weinberg, M. D. DePiero, and J. A. Miola, "The Silicon Oscillating Accelerometer: A MEMS Inertial Instrument for Strategic Missile Guidance," *Missile Sciences Conference*, Monterey, CA, pp.44-51, Nov. 7-9, 2000.

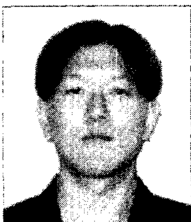

Illhwan Kim He received the B.S. degree in Electrical Engineering of Korea Advanced Institute of Science and Technology in 2002, and the M.S. degree in Electronical Engineering of Seoul National University in 2004. He is in the Ph.D candidate in Seoul National University, researching in the areas of MEMS devices.

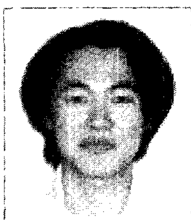

Seonho Seok He received the B.S. degree in electrical engineering from the Kyung pook National University in 1997 and the M.S. and Ph.D. degrees in electrical engineering from the Seoul National University in 1999 and 2004, respectively. He is an post-doctor in IEMN(Institut d'Electronique de Microelectronique et de Nanotechnologie), France.

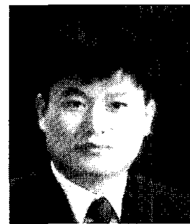

Hyeon Cheol Kim He received the B.S., M.S., and Ph.D. degrees in electronics engineering from Seoul National University in 1990, 1992, and 1998, respectively. From 1998 to 2001, he worked as an member of research staff of Samsung Advanced Institute of Technology. From 2001 to 2003, he worked as an senior engineer of Chromux Technology Inc. He joined the faculty of Seoul NationalUniversity in 2004, where he is currently an BK21 Fund Professor in the School of Electrical Engineering.

Moon Koo Kang He received the B.S., M.S., and Ph.D. degrees in mechanical engineering from Seoul National University in 1991, 1993, and 1997, respectively. From 1997 to 1998, he worked as an post-doctor of Univ. of California Los Angeles. From 1998 to 2000, he worked as an special researcher in Institude of Advanced Machinery and Design of Seoul National University. He joined the faculty of Seoul NationalUniversity in 2001, where he is currently an BK21 Fund Professor in the School of Electrical Engineering.

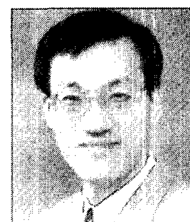

Kukjin Chun He received the B.S. degree in Electronics Engineering from Seoul National University in 1977 and the M.S. and Ph.D. degrees in Electrical Engineering from the University of Michigan in 1981 and 1986, respectively. He was an Assistant Professor in the Department of Electrical and Computer Engineering at Washington State University from 1986 to 1989. He joined the faculty of Seoul National University in 1989, where he is currently a professor in the School of Electrical Engineering. He is a Senior Member of IEEE and a Life Member of IEEK. He has been a director of Center for Advanced Transceiver System since 2000, which develops RF front-end solution for next generation wireless communication system. He is also a director for Inter-university Semiconductor Research Center at Seoul National University since 2005. His research interests include integrated sensors, intelligent Microsystems and MEMS processing technologies.